



Design and Construction of Ultraviolet and Incoming Solar Irradiance Sensing Device

Osinowo M. Olatunde^{1*}, Willoughby A. Alexander¹, Dairo O. Feyisayo¹, Ewetumo Theophilus² and Kolawole L. Babatope¹

¹Department of Physical Sciences, Redeemer's University, Ede, Osun State, Nigeria

²Department of Physics with Electronics, The Federal University of Technology, Akure, Nigeria.

Received: 29/9/2020

Accepted: 7/10/2021

Published: 30/12/2022

Abstract

In-situ measurements of ultraviolet (UV) and solar irradiance is very sparse in Nigeria because of cost; it is estimated using meteorological parameters. In this work, a low-cost UV and pyranometer device, using locally sourced materials, was developed. The instrument consists of a UV sensor (ML8511), a photodiode (BPW34) housed in a carefully sealed vacuumed glass bulb, the UV and solar irradiance sensor amplifiers, a 16-bit analog-to-digital converter (ADS1115), Arduino mega 2560, liquid crystal display (LCD) and microSD card for data logging. The designed amplifier has an offset voltage of 0.8676 mV. The sensitivity of the irradiance device is 86.819 Wm⁻²/mV with a correcting factor of 27.77 Wm⁻² and a maximum range of 1200 Wm⁻². The instrument validation error is 9.67% and a correlation coefficient of 0.89 when compared with a standard SRS100 pyranometer. The UV sensor showed a close response with a correlation of 0.99 in comparison with a standard Skye instrument. From 08:00 to 16:00 local time (LT), there is a very close agreement between the standard device and the developed counterpart, with marginal differences of about 9.6% observed at the two extremes.

Keywords: Ultraviolet, solar irradiance, transimpedance amplifier, Arduino data logger, Photodiode

Introduction

Solar ultraviolet (UV) radiation at the earth's surface has both beneficial and adverse effects on human health [1], [2]. For instance, UV radiation is a principal source of vitamin D, while the excess of UV exposure is a risk factor for immune suppression, cataracts and skin cancers. Action spectra [6] typically characterise the wavelength dependence of these effects. The most widely used is the standardized action-spectrum for erythema, otherwise known as the CIE (Commission Internationale de l'Eclairage) spectrum [3]. There are also other action spectra related to skin cancer and melanoma [1], [4], [5].

On top of the atmosphere, solar radiation is distributed in spectral form [6], [7]. The radiation on earth can be in two forms either directly from the sun's disk, known as direct-beam radiation, or after scattering and being absorbed by constituents of the atmosphere as diffuse radiation [7]. The global or total solar radiation is the sum of direct and diffuse radiations. The relative path length of the sun's direct beam (when directly overhead) through the atmosphere is known as air mass and this is the same as the secant of the solar zenith angles that are less than 60° [8], [10]. If the direct beam travels a longer path length in the air,

*Email: osinowom@run.edu.ng

the air mass increases with a lot of absorption and scattering. This creates more scattering in the shorter wavelengths range (ultraviolet and visible) [9], [10].

This work aims to develop a low-cost UV and incoming solar irradiance measuring device incorporating a data logger that can be used to study these parameters at any location.

Materials and methods

A. Solar Radiation Sensor Using a Photodiode

Photodiodes and phototransistors are electronic devices that can be used to measure light intensity and solar irradiance within the electromagnetic spectrum. An electrical signal is generated in the form of current or voltage, which is proportional to the light intensity of solar irradiance that fall on their windows. A BPW34 photodiode was used as a solar irradiance sensor. This diode has a bandwidth of 430 nm to 1100 nm [11], making it suitable as a transducer for irradiance measurements. When used as light or radiation sensor, photodiodes are operated in photoconductive mode around a low input bias current operational amplifier called transimpedance amplifier (TIA) as connected in Figure 1a. When exposed to a source of light or solar radiation, a reverse photo current I_{pd} , flows through the diode. This I_{pd} varies in the microamp range which depends on the intensity of the light falling on the diode's p-n junction at any instant. and it causes an increase in the output voltage of the op-amp such that $V_{out} = -I_{pd} R_f$. In the absence of I_{pd} , the voltage at the non-inverting input of the amplifier appears at the amps output but if this pin is grounded it settles at zero volts.

To prevent output saturation by the amplifier, the non-inverting input is biased with a low voltage divider formed by R_1 and R_2 which is equal to 0.1 V. R_f and C_1 form a pole within the amplifier's bandwidth. Combinations of R_3 and C_3 form a low pass filter at the output. The amplifier was built on a strip board (Figure 1b) while the diode was encased in a glass dome with silica gel to absorb moisture inside the dome as shown in Figure 2. The amplifier was inserted inside a one-inch pressure pipe that holds the sensor. Figure 3 shows the final image of the device and its installation outside for recordings.

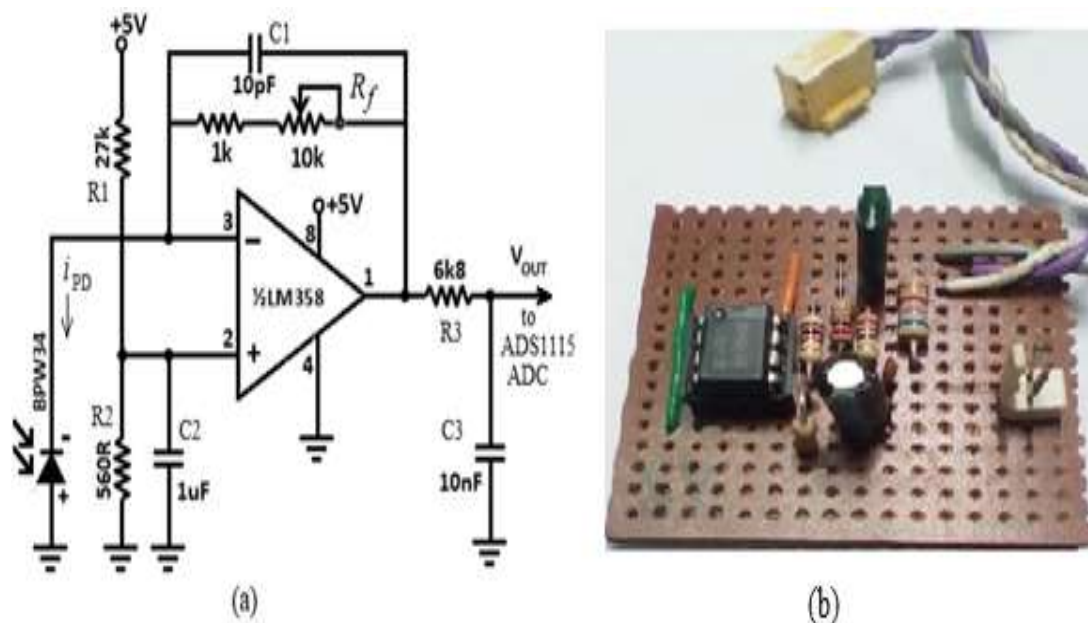


Figure 1: (a) Transimpedance amplifier (TIA) circuit and (b) The assembled amplifier



Figure 2: The photodiode enclosed in an evacuated electric bulb

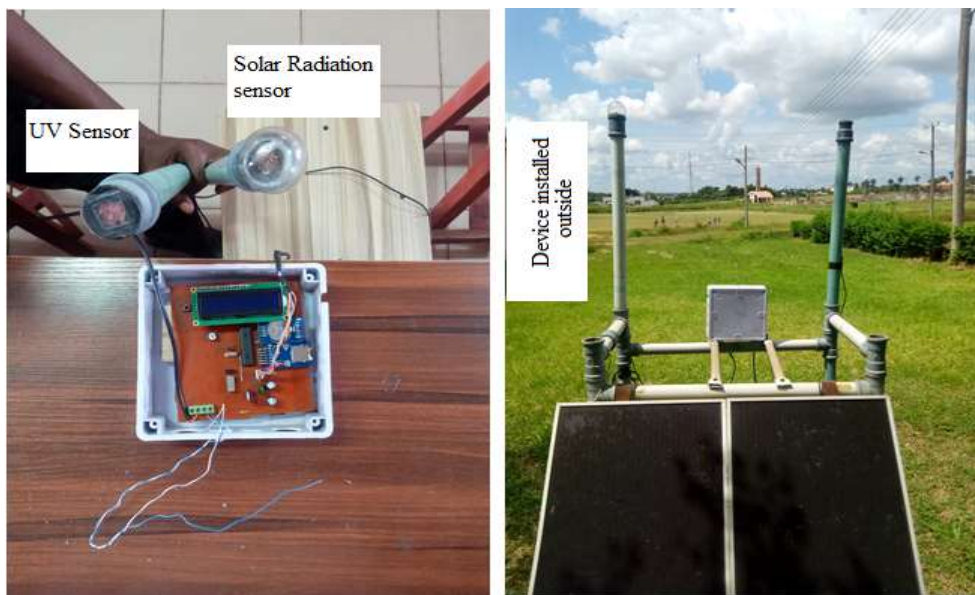


Figure 3: Image of the device and the installation outside

In a TIA design, the operational amplifier’s output voltage fluctuation range must be defined, so as to determine the feedback resistor and capacitor values that will be used to calculate the amplifier’s phase margin and gain. The components in the circuit of Figure 1a were realised using the characteristics of the photodiode sensor through the following steps [12]:

a) Selection of the gain resistor (R_f)

$$R_f = \frac{V_{OUT(max)} - V_{OUT(min)}}{I_{pd(max)}} \quad (1)$$

b) Feedback capacitor (C_1) to meet the circuit’s bandwidth

$$C_1 = \frac{1}{2\pi R_f f_p} \quad (2)$$

c) Determination of bias network for a reference voltage (V_{ref}) of 0.1 V

$$R_1 = \frac{V_{cc} - V_{ref}}{V_{ref}} R_2 \quad (3)$$

Where: I_{pd} = photodiode reverse current; $R_f + 1k$ = feedback gain resistor; C_1 = feedback capacitor; f_p = amplifier's pole frequency response; R_1 and R_2 are bias resistors.

Frequency response and stability of the amplifier are enhanced by combinations of C_1 and R_f . According to BPW34 specifications given in Table 1, the passive components required to achieve the desired amplification are given in Table 2. The output pin 1 of the TLC272 op-amp in Figure 1a is connected to the ADS1115, a 16-bit analog-to-digital converter (ADC).

Table 1: Characteristics of BPW34

$I_{in(min)}$	$I_{in(max)}$	$V_{o(min)}$	$V_{o(max)}$	Bandwidth (BW)	V_{cc}	V_{ee}	V_{ref}
0 A	75 mA	3 V	0.1 V	20 kHz	5 V	0 V	0.1 V

Table 2: Passive components requirements

R_f	R_2	R_3	C_1	C_2	C_3
36.66 k Ω	27.44 k Ω	560 Ω	10 pF	1 μ F	10 nF

The ADS1115 is a precision, low power ADC with ease of implementation and it features an onboard reference voltage with an oscillator. Data are exchanged via an inter-integrated circuit (I²C) serial interface with four selectable slave addresses. It can be operated with 2.5 V to 5.5 V with higher conversion rates at about 860 samples in one second (SPS). It also comes with an amplifier that can be programmed for different gains with input as low as ± 256 mV. Its four-input multiplexer circuit can provide four single inputs or two differential inputs and it can operate either as single-shot or continuous conversion modes.

B. UV Sensor ML8511

The ML8511 is an ultraviolet radiation sensor that is sensitive to UV-A and UV-B, which is suitable for acquiring ultraviolet intensity both outdoors and indoors. ML8511 comes with an internal amplifier that converts the photo-current from the ultraviolet photodiode to analog voltage in proportion to the ultraviolet intensity. This output voltage can easily be fed to an ADC and then to a microcontroller for further processing. Internal circuit of ML8511 is shown in Figure 4 [13].

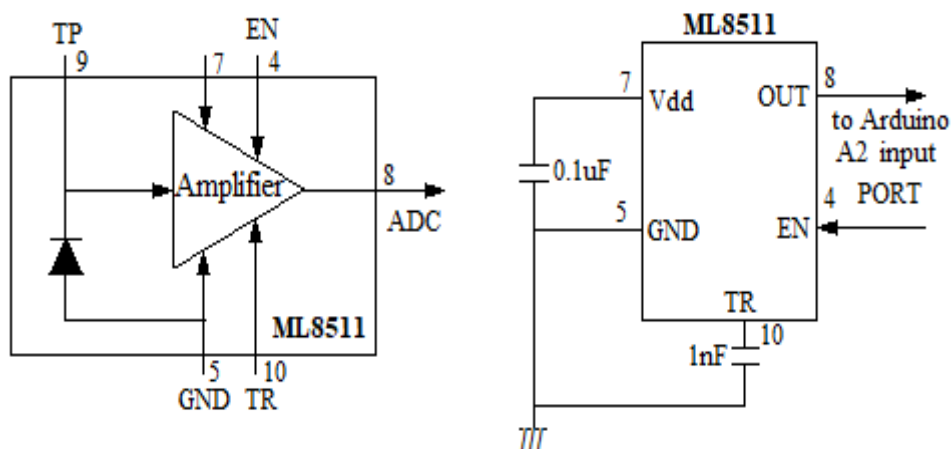


Figure 4: Internal and biasing circuits of ML8511

C. Data Logging Unit

To record data with date and time stamp, a DS3231 and AT24C32 are I²C implemented as precision Real Time Clock (RTC) module which communicates with Arduino2560 via serial clock (SCL) and serial data (SDA) buses. The RTC module records and saves the year, month, day, hours, minutes and seconds. The module incorporates a 3.3 V lithium battery and maintains accurate time keeping even when the main power supply is disconnected. The interface between the ATmega2560 and the microSD card module is achieved by means of the high-speed SPI communication bus, capable of supporting simultaneous data transfer in master to slave directions and vice versa. The card module supports microSD Card or microSDHC card (a high-speed card) with voltage level conversion circuit that can interface 5 V or 3.3 V levels. Communication interface is via a standard SPI interface control. The SPI interface has a total of six pins (GND, VCC, MISO, MOSI, SCK, and CS): GND to negative and VCC is the power supply, MISO, MOSI, and SCK pins are the SPI bus; chip select pin is SC, MISO (master in slave out) and MOSI (master out slave in) signals are also converted to 3.3 V, which general AVR microcontroller systems can read. These pins are well defined in the microcontroller program for proper communications to record the data on a memory card, and to be downloaded and viewed in .csv or excel (.xls) format.

Calibration and examination of sensors

A. Solar irradiance calibration

The solar irradiance amplifier after construction was tested by connecting it to a resistive attenuator circuit of Figure 5. This attenuator circuit drops the output voltage to millivolts range. A linear potentiometer of 5 k Ω was used to change the value from the maximum of the range selected. The performance of the amplifier is shown in Figure 6. The amplifier gave a linear response, and from the graph an empirical formula obtained shows that the amplifier has a background voltage of 0.8978 mV (intercept on the mV output) which is due to the amplifier's offset voltage. The photodiode and the amplifier were set up and placed in an open environment unobstructed alongside a standard SRS100 pyranometer. The two sensors' output voltages (mV) and the solar irradiance (Wm⁻²) were then obtained. The relationship between the two sensors was plotted as in Figure 7. An empirical equation was obtained as shown in the plot of Figure 7 to convert the developed pyranometer's voltage output to equivalent solar irradiance (Wm⁻²).

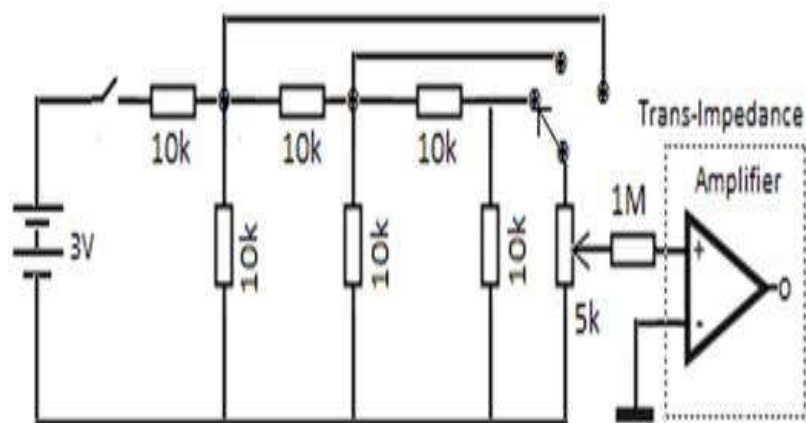


Figure 5: Attenuator network for calibration of irradiance sensor

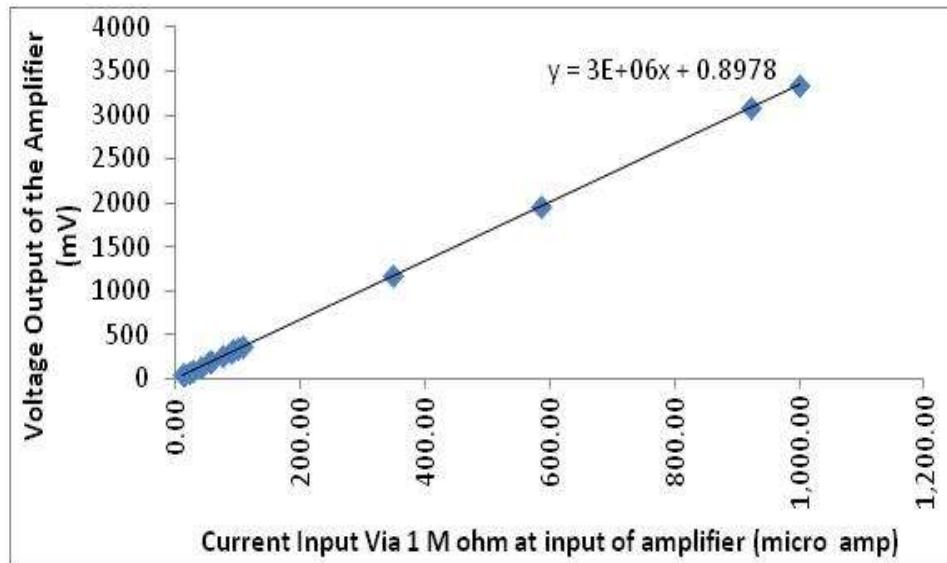


Figure 6: Solar irradiance sensor amplifier's response

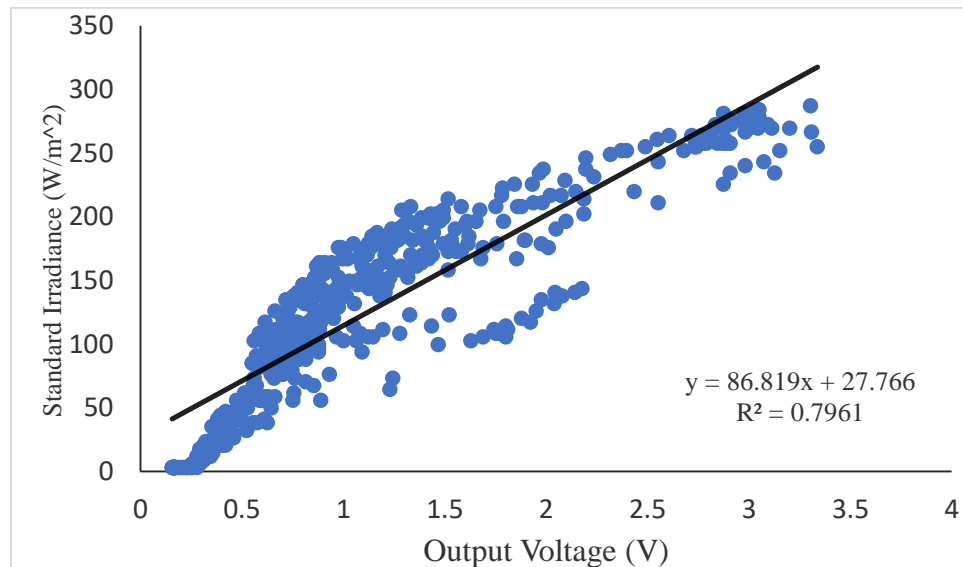


Figure 7: Standardising the developed sensor with SRS100

The developed low-cost pyranometer was deduced to have a sensitivity of $8.6819 \text{ Wm}^{-2}/\text{mV}$ without amplifier. A correcting factor of 27.77 Wm^{-2} was obtained from the standardisation of Figure 8 using SRS100 as a standard pyranometer. Also, the maximum output voltage of the amplifier was pegged at 4 V in order not to exceed the required 5 V for the Arduino input. The instrument was placed in the observatory after calibration for many weeks, and the result obtained showed a good agreement with that of SRS100 except at early hours of the day around 7:00 LT to 8:30 LT and around 17:30 LT onwards. The correlation is about 0.89 and 9.67 % error using the data obtained on August 12, 13 and 14, 2018. The frequency response of this sensor ranged from 430 nm to 1100 nm.

B. Ultraviolet sensor

Sensitivity of the photodiode on ML8511 covers UV-A and UV-B range with embedded operational amplifier that gives analog output voltage. The sensor was calibrated from the

manufacturer but it was also examined for its accuracy and compared with the Skye Instrument at the Department of Meteorology, Federal University of Technology Akure (FUTA), Nigeria. The instrument developed was placed beside the Skye Instrument at FUTA and results were plotted as shown in Figure 8. Both plots exhibited a good concurrence with a correlation close to unity of 0.99. The re-standardization in Figure 9 gave the slope of 0.998 and error presence is 0.0102 mWm^{-2} .

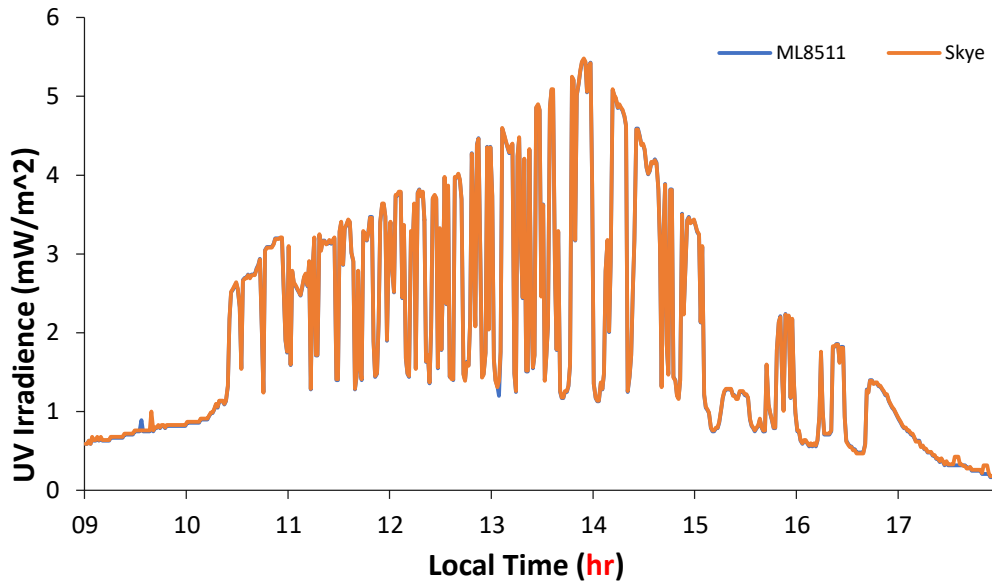


Figure 8: Comparison of UV irradiance measurements from ML8511 and Skye Instrument

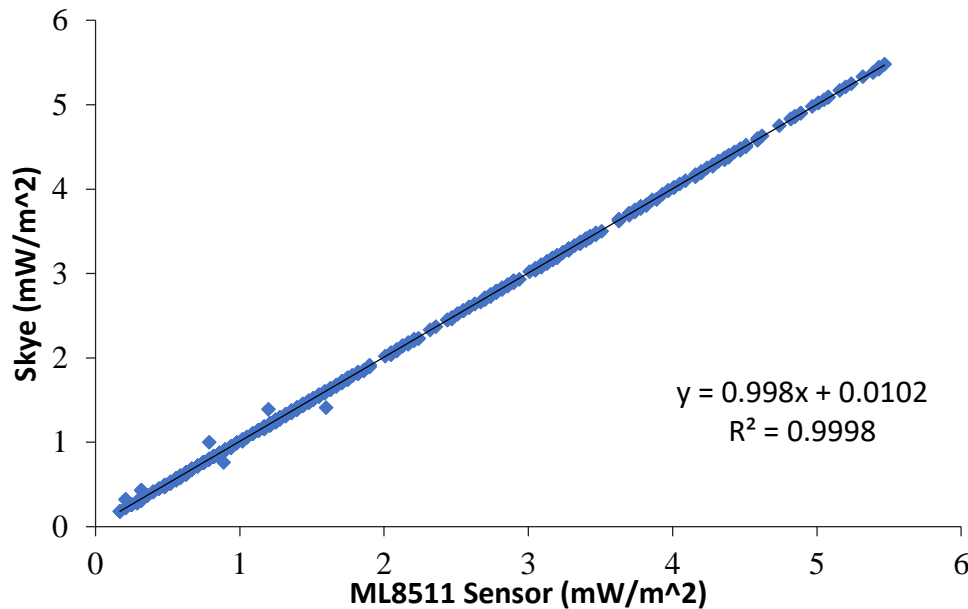


Figure 9: The standardisation of the UV data from ML8511 using the Skye Instrument

Results and discussion

The developed sensor and SRS100 were examined by placing the two in the meteorological observatory at the Redeemer’s University, Ede, Nigeria. The instrument was placed outside in the observatory after calibration for many weeks. The result obtained showed a good agreement with the SRS100 except in the early hours of days when the sun

rise intensity is above 50% and sun set intensity is below 50% from 7:00 LT to 8:30 LT and around 17:30 LT downward respectively as shown in Figures 10-13 for some days in August 2018. From the plots, the same trends and variations were observed with slight differences that may be due to individual responses of the sensors or the amplifiers' responses and their slew rates. Average correlation value between the irradiance sensor and SRS100 is 0.89 with an error of 9.67% when compared with each other. The spectra wavelength of the developed sensor ranged from 430 nm to 1100 nm. Also, the UV irradiance sensor, ML8511, consisting of A and B components of ultraviolet irradiance. Figures 8 and 9 show the standardization and comparison of ML8511 with a standard Skye UV instrument respectively. The comparison shows excellent close agreement with a correlation coefficient of 0.99. The slope of the standardization plot of Figure 9 is 0.998 with an error of 0.0102 mWm^{-2} . The UV variation plot on 12 August 2018 is shown in Figure 14. This displays good response for the particular day at Ede, Nigeria.

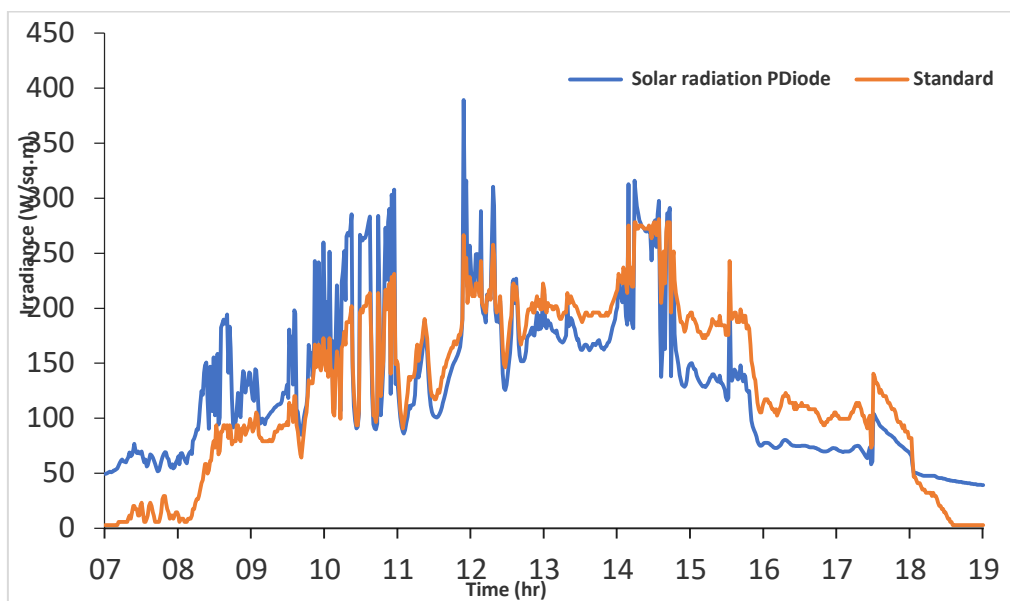


Figure 10: Variation solar irradiance on August 12, 2018

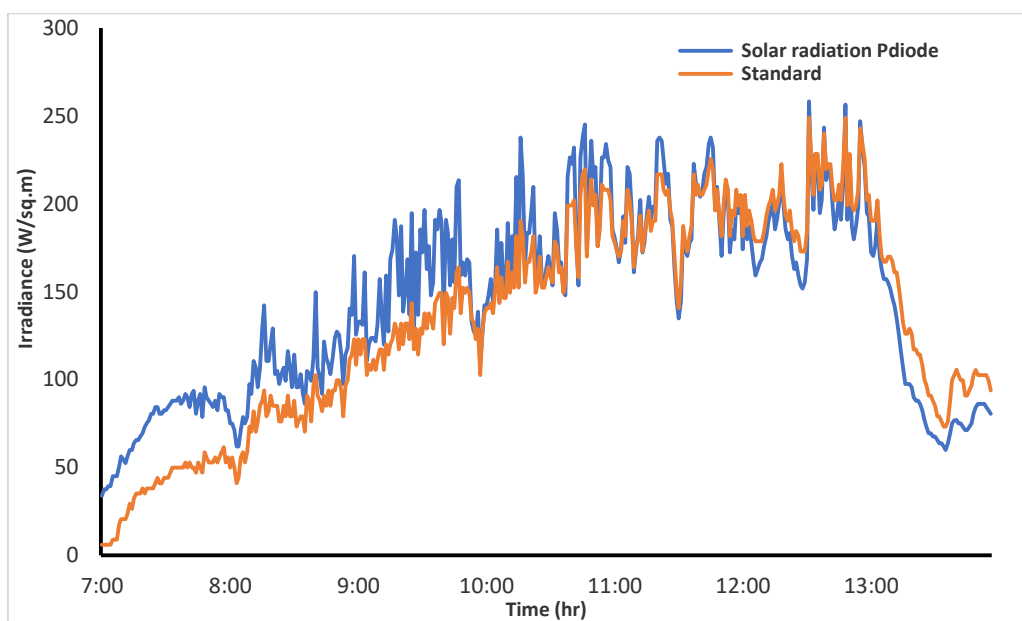


Figure 11: Variation solar irradiance on August 13, 2018

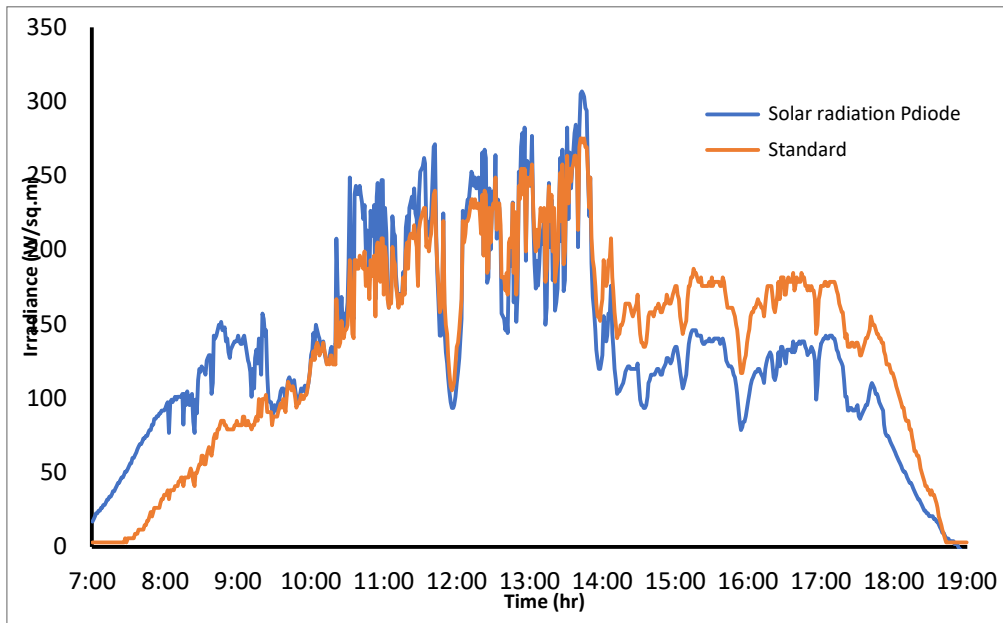


Figure 12: Variation solar irradiance on August 14, 2018

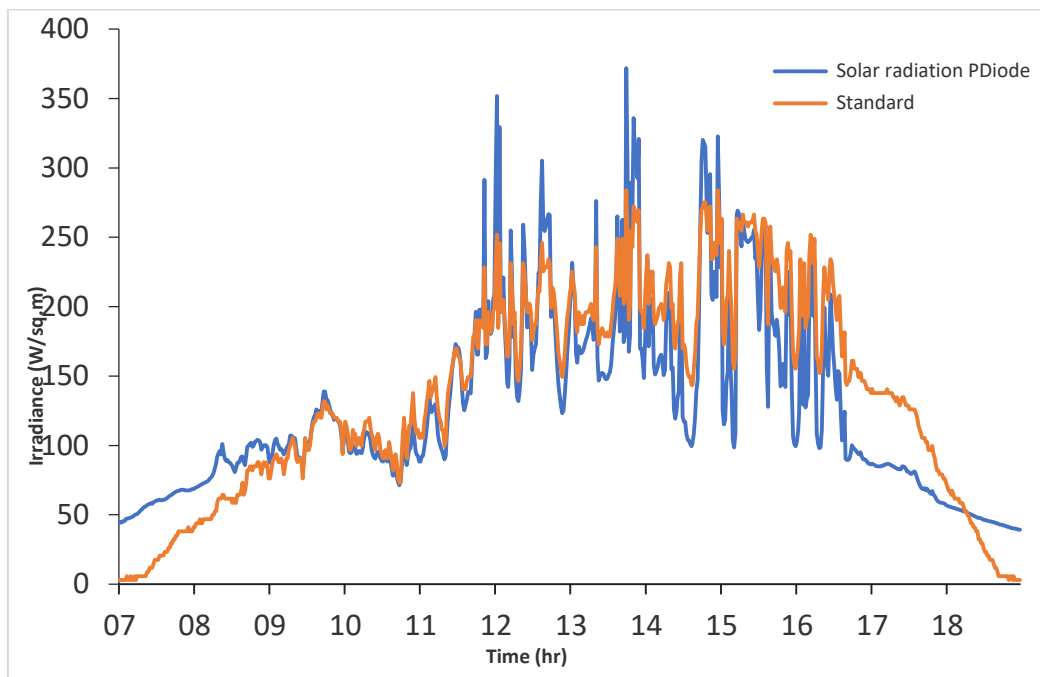


Figure 13: Variation solar irradiance on August 15, 2018

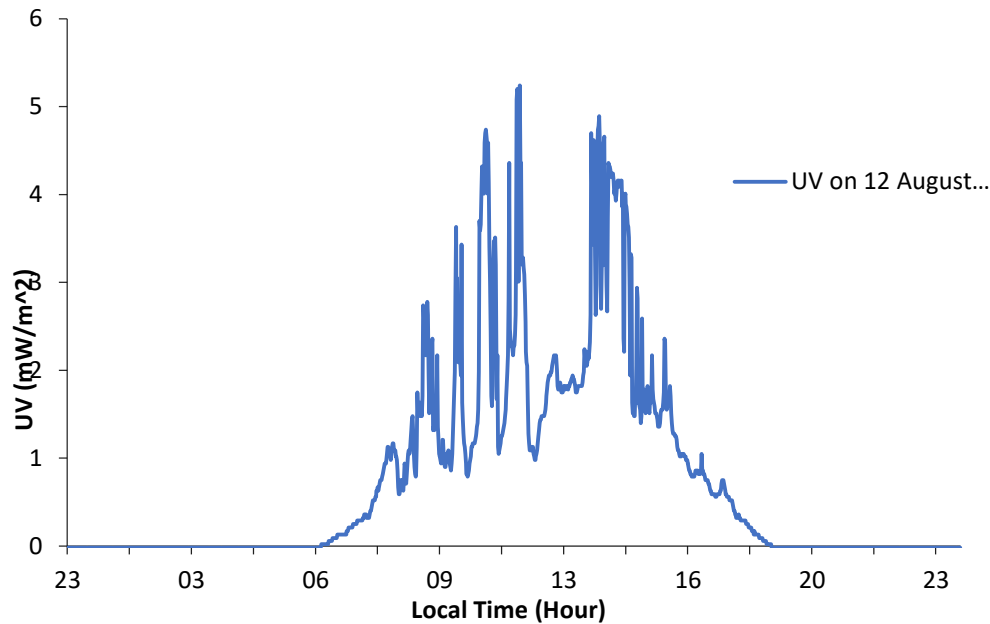


Figure 14: Variation of UV irradiance at Ede, Nigeria on 12 August 2018

Conclusions

The developed instrument is a dual-purpose device designed for measuring UV and solar irradiance. The constructed UV measuring device displayed excellently, close agreement with the standard Skye instrument, exhibiting a correlation of 0.99. Similarly, the BPW34 irradiance sensor exhibited a sensitivity of $86.92 \text{ Wm}^{-2}/\text{mV}$ and a close agreement with SRS100 pyranometer with correlation of 0.89. The cost of developed device is less than 69 % when compared with Skye instrument. This work has developed an affordable and easy to install UV and solar radiation measuring device.

References

- [1] W. W. Nyamsi, M. R. A. Pitkänen, Y. Aoun, P. Blanc, A. Heikkilä, K. Lakkala, G. Bernhard, T. Koskela, A. V. Lindfors, A. Arola and L. Wald, "A new method for estimating UV fluxes at ground level in cloud-free conditions," *Atmos. Meas. Tech.*, vol. 10, no. 12, pp. 4965–4978, Dec. 2017.
- [2] A. Juzeniene, P. Brekke, A. Dahlback, S. Andersson-Engels, J. Reichrath, K. Moan, M. F. Holick, W. B. Grant and J. Moan, "Solar radiation and human health," *Rep. Prog. Phys.*, vol. 74, no. 6, pp. 066701, May 2011.
- [3] A. F. McKinlay and B. L. Diffey, "A reference action spectrum for ultraviolet induced erythema in human skin," *CIE J.*, vol. 6, pp. 17–22, Jan. 1987.
- [4] R. B. Setlow, E. Grist, K. Thompson and A. D. Woodhead, "Wavelengths effective in induction of malignant melanoma," *P. Natl. Acad. Sci. USA*, vol. 90, pp. 6666–6670, 1993.
- [5] F. R. de Gruijl, H. J. Sterenborg, P. D. Forbes, R. E. Davies, C. Cole, G. Kelfkens, H. van Weelden, H. Slaper and J. C. van der Leun, "Wavelength dependence of skin cancer induction by ultraviolet irradiation of albino hairless mice," *Cancer Res.*, vol. 53, pp. 53–60, 1993.
- [6] C. Wehrli, "Extraterrestrial Solar Spectrum," *World Radiation Center*, Davos Dorf, Switzerland, Pub. No. 615. 1985.
- [7] C. J. Riordan, R. L. Hulstrom and D. R. Myers, "Influences of Atmospheric Conditions and Air Mass on the Ratio of Ultraviolet to Total Solar Radiation," *Sol. Energy Res. Inst. (SERI)*, USA. pp. 1-4, 1990.

- [8] WHO, "Global Solar UV Index - A practical guide," World Health Organization, Geneva, Switzerland, WHO no. WHO/SDE/OEH/O2.2., ISBN. 9241590076, 2002 [Online]. Available: <https://www.who.int/publications/i/item/9241590076>.
- [9] F. Kasten and A. T. Young, "Revised Optical Air Mass Tables and Approximation Formula," *Appl. Optics*, vol. 28, no. 22, pp. 4735-4738, Nov. 1989.
- [10] A. Webb, J. Gröbner and M. Blumthaler, "A practical guide to operating broadband instruments measuring erythemally weighted irradiance," *EU Publications Office*. No. EUR22595, COST-726, 2006.
- [11] Vishay, "BPW34: Silicon PIN Photodiode," Vishay datasheet, rev. 2.1, no.81521 - 91000, rev. Jan. 2022. [Online]. Available: <https://www.vishay.com/docs/81521/bpw34.pdf>.
- [12] J. Caldwell, "1 MHz, Single-Supply, Photodiode Amplifier ReferenceDesign," TI Application Note TIDU535, pp. 1-19, Nov. 2014.
- [13] ML8511 Datasheet 2013. "UV Sensor with Voltage Output," ML851, no. FEDL8511-05, LAPIS Semiconductor Co. Ltd., Japan, Mar. 2013 [Online]. Available: [https://cdn.sparkfun.com / datasheets/Sensors/LightImaging/ML8511_3-8-13.pdf](https://cdn.sparkfun.com/datasheets/Sensors/LightImaging/ML8511_3-8-13.pdf)